Purdue University
Purdue e-Pubs

International Refrigeration and Air Conditioning Conference

School of Mechanical Engineering

2016

Transient Modeling of a Thermosiphon based Air Conditioner with Compact Thermal Storage: Modeling and Validation

Rohit Dhumane
University of Maryland, United States of America, dhumane@umd.edu

Yilin Du
University of Maryland, United States of America, duyilin@umd.edu

Jiazhen Ling
University of Maryland, United States of America, jiazhen@umd.edu

Vikrant Aute
University of Maryland, United States of America, vikrant@umd.edu

Reinhard Radermacher
University of Maryland, United States of America, raderm@umd.edu

Transient Modeling of a Thermosiphon based Air Conditioner with Compact Thermal Storage: Modeling and Validation

Rohit Dhumane[1], Yilin Du[1], Jiazhen Ling[1], Vikrant Aute[1]*, Reinhard Radermacher[1]

Center for Environmental Energy Engineering, University of Maryland, College Park, 4164 Glenn L. Martin Hall Bldg., MD 20742, USA
Tel.: +1 301 405 8726, E-mail address: vikrant@umd.edu

* Corresponding Author

ABSTRACT

The Roving Comforter (RoCo) is an innovative personal thermal management technology currently being developed at the University of Maryland as part of Advanced Research Projects Agency – Energy (ARPA-e) project. Among several system configurations of RoCo, the paper focuses on a miniature battery-powered vapor compression cycle (VCC) system fitted on a remote-controlled robotic platform. The heat rejected from the condenser during its operation is stored in a compact phase change material (PCM) based heat storage device. Once the PCM storage reaches full capacity, it needs to be recharged. The PCM heat exchanger needs to be designed so that the melting PCM captures the heat generated during the VCC operation and then re-solidifies again with minimal energy usage during the its recharge mode. The thermosiphon operates through the same refrigerant circuit by bypassing certain components like the compressor to reduce flow resistance. Thus the circuit is designed to operate as a VCC during the cooling mode and as thermosiphon during the recharge mode. The VCC needs to have a high coefficient of performance (COP) while the thermosiphon needs to solidify PCM material at highest possible rate. To capture the time-dependent behavior of solidification, transient modeling of thermosiphon is desired. The prototype developed has a COP of 2.85 and needs roughly 8 hours to recharge the thermosiphon. Comparison of modeling results with the experimental data have been provided to validate the model. Several cases of RoCo thermosiphon are then simulated for different PCM using the model to select the most suitable PCM.

1. INTRODUCTION

Heating and cooling of buildings accounts for 13% of US primary energy consumption and 13% of domestic greenhouse gas emissions. A large amount of energy is consumed by air-conditioning systems to maintain space temperature within a narrow and uniform range of 70°F to 75°F, neither of which is really necessary for thermal comfort. Local thermal management systems (LTMS) modify the local thermal environment around the occupant(s) as per their comfort. Thus it enables elevation of typical building set point temperature range leading to energy savings of at least 15% for a 4°F set point elevation (Hoyt et al, 2005). High costs and efforts are the main deterrents for adaption of improved air conditioning technology. As a result, buildings typically replace their air-conditioning technology in periods anywhere between 10 to 25 years. Hence a very low cost, LTMS device with a good consumer appeal has a very high potential towards large scale energy savings.

Through the review of current LTMS products, it is found that they are typically expensive, bulky, have limited mobility, short operating times and mediocre consumer appeal. The Roving Comforter (RoCo) is designed to address these limitations. It is a personal attendant for thermal comfort and operates by blowing air at desired temperature through robotically controlled nozzles at right locations on human body. It is highly portable and can follow a person as an autonomous robot. For its cost targets, it has a goal of a 3-year payback period including both capital and operational costs.

Several concepts were proposed (Dhumane, 2016) to meet the design criteria and finally vapor compression cycle (VCC) based system with a compact thermal storage was chosen based on efficiency and weight. The compact thermal storage is made using a paraffin based phase change material (PCM) enclosing the condenser coils. The amount of phase change material is calculated after incorporating safety factors to capture 170 W of heat for two hours of continuous operation. The cycle operation will be terminated after the PCM is completely melted and it needs to be re-solidified before providing cooling again. The system is transformed by minor adjustments to operate as a thermosiphon to solidify the phase change material. The thermophysical behavior of both these modes of operations is very complex and to understand and optimize their performance detailed modeling is required.

Transient modeling of both modes of operation were carried out using Modelica for its ability to solve complicated dynamic system models. The components of basic VCC are obtained from the work of Qiao et al. (2015). New components like phase change material based heat exchanger (PCM HX), thermosiphon's downcomer and riser are developed to enable simulation of both modes of operation. The results of VCC mode of operation are presented in Dhumane (2016) and this paper focuses only on the thermosiphon mode.

2. SYSTEM DESCRIPTION

RoCo as a system is a small battery-powered VCC mounted on a robotic platform for its motion. A fan blows air over the evaporator which is directed by nozzles on the individual. Since RoCo is a portable device, it needs to store the condenser heat generated during the VCC operation. This is accomplished by enclosing the condenser in a PCM with appropriate melting temperature, so as to operate with a good coefficient of performance. The cooling operation is terminated when the PCM is fully melted. This stored waste heat needs to be discharged before RoCo can deliver cooling again. A gravity assisted thermosiphon operation is carried out to re-solidify the PCM. This mode referred to as the recharge mode is enabled by bypassing the compressor and expansion valve using ball valves to reduce flow resistance for the refrigerant. This process is to be carried outside the conditioned space once the ambient is preferable (like at night). RoCo will automatically reach this charging place after its thermal storage is fully saturated. The schematic for both VCC and thermosiphon mode of operation are shown in Figure 1. The mass of the refrigerant (R134-a) required for operations of VCC and thermosiphon are different. To manage the refrigerant charge, a receiver is included in the circuit to store the additional charge during the cooling mode.

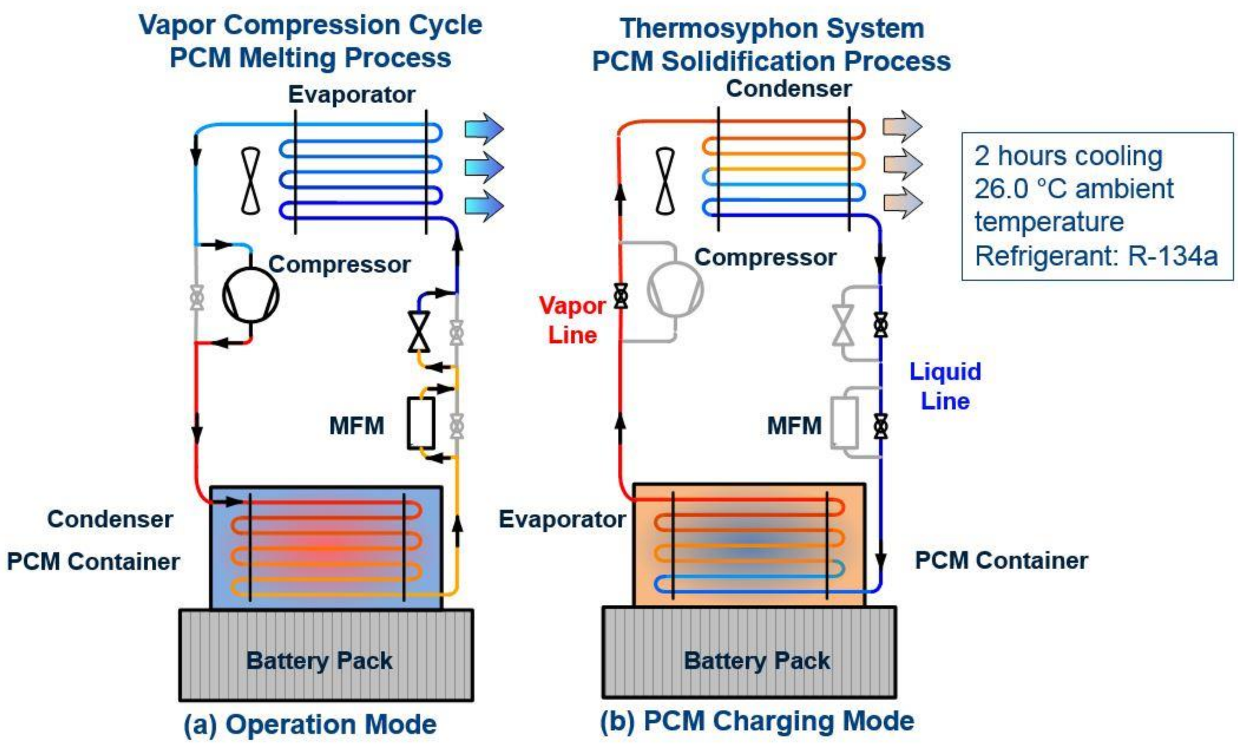

Figure 1: The two modes of operation of RoCo

The compact VCC system powering the RoCo is sized to deliver 170 W of cooling. It draws in room air at temperature of 26°C. The mean exit air temperature is measured to be 22.7°C. The maximum weight of the system permitted is 30 kg. The total mass of PCM used is 7.8 kg. The condenser of the vapor compression cycle in the cooling mode consists of four refrigeration tubes which are spiraled inside the cylindrical shaped phase change material container as shown in Figure 2.

The runtime for the thermosiphon mode to solidify the molten PCM is 8 hours for the current prototype with a fan blowing air over the airside heat exchanger.

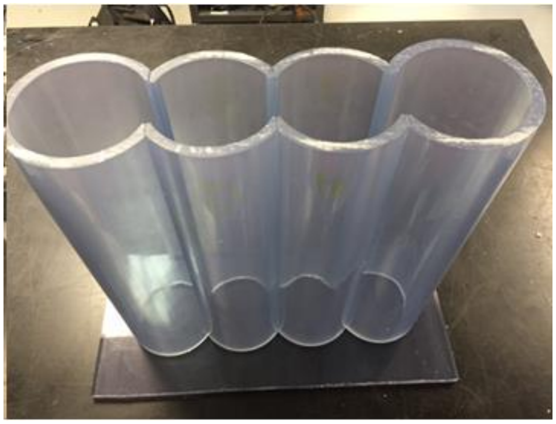

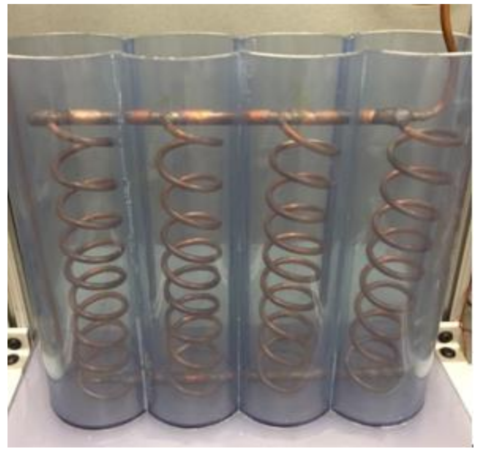

Figure 2: Condenser made from spiral tube placed inside PCM container

3. PHASE CHANGE MATERIAL MODELING

Solving three dimensional conduction problem with spiral shaped refrigerant tube inside the PCM container while obtaining the transient behavior of the VCC is complicated and computationally costly. Hence, a one dimensional problem which solves a simpler problem is modeled. The refrigerant tube is assumed to be straight but equal in length to the spiral tube. The total weight of the PCM surrounding this straight tube is kept the same as in the prototype. Hence the total weight of the PCM per unit length of the refrigerant tube is same for the model and the prototype. Cylindrical coordinate system with finite volume discretization is used in modeling.

Leonhardt and Muller (2009) have described the modeling of residential heat pump system which uses PCM for heat storage. Their method uses an arc tangent function to describe the specific enthalpy behavior of PCM across the solid liquid boundary. However, the heat pump model is implemented using empirical data obtained from manufacturers limiting their application to the specific model.

While trying to capture the two phase behavior using their model, the energy storage term which is the product of density, specific heat capacity as well as temperature in the energy equation, contained all three terms as variables. This lead to challenges in obtaining solutions for the equation. As a result, the current work uses formulation of Stefan problem as outlined in Alexiades and Solomon (1993). This method however, does not capture the temperature glide which occurs in melting of paraffin based PCM and assumes a fixed melting point.

Figure 3 shows the cross section of the PCM block with the assumption of straight refrigeration tube. The PCM volume is then discretized into multiple finite volume blocks.

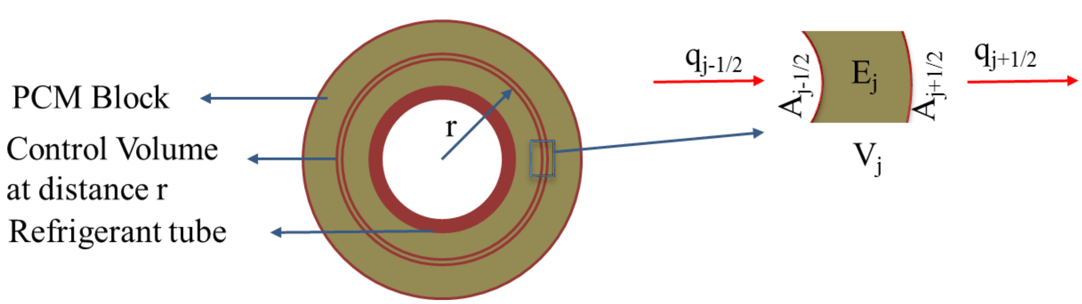

Figure 3: Finite Volume Discretization of PCM Block

The mathematical problem is described as:

Find $T(x,t)$ such that

$\frac{\partial(\rho c_p T)}{\partial t} = \frac{1}{r}\frac{\partial}{\partial r} rk \frac{\partial T}{\partial r}$	For	$r_i < r < r_o$	(1)
$T(r,0) = T_{init}$	Initial Condition	$r_i \leq r \leq r_o$	(2)
$T(r_i,t) = T_t$	At the inner radius of the PCM block, the temperature is that of the refrigerant tube		(3)
$\frac{\partial T(r_o,t)}{\partial r} = 0$	The outer radius of the PCM block is assumed to be fully insulated and hence adiabatic boundary condition		(4)

Enthalpy solution method is used to solve equations 1-4. Finite volume discretization of equation 1 gives equation 5. The location of the terms of equation 5 in the grid is shown in Figure 3. The surface areas and heat fluxes are calculated at the boundary while the energy density and volume are at the center of the grid. The areas and volume are calculated by standard formulae for annulus with profile given in Figure 3.

$$E_j^{n+1} = E_j^n + \frac{\Delta t}{\Delta V_j}\left(q_{j-\frac{1}{2}}^n A_{j-\frac{1}{2}} - q_{j+\frac{1}{2}}^n A_{j+\frac{1}{2}}\right) \tag{5}$$

The heat flux calculation is carried out by using Kirchoff temperatures transformations since they treat mushy nodes as isothermal. This is shown in equations (6) and (7).

$$u = \begin{cases} k_s[T - T_m], & if\ T < T_m \\ 0, & if\ T = T_m \\ k_L[T - T_m], & if\ T > T_m \end{cases} \tag{6}$$

$$q_{j-\frac{1}{2}} = \frac{u_{j-1} - u_j}{\Delta r} \tag{7}$$

The process of melting is handled by a simple switching scheme given by equation 8. Thus the phases are determined by enthalpy alone. The zero for the enthalpy is set for the point when melting starts as mentioned in equation 8.

$$T_j^n = \begin{cases} T_m + \dfrac{E_j^n}{\rho c_s}, & if\ E_j^n \leq 0\ (solid) \\ T_m, \ if\ 0 < E_j^n < \rho L\ (interface) \\ T_m + \dfrac{E_j^n - \rho L}{\rho c_L}, if\ E_j^n \geq \rho L\ (liquid) \end{cases} \tag{8}$$

The model does not incorporate volume expansion and hence average value of densities of both phases is used for calculations. The decrease in density is 9% in the material used and hence it is a reasonable assumption.

4. THERMOSIPHON MODELING

To model the behavior of thermosiphon, only downcomer and riser are the new components which needed to be modeled. This reflects the benefit of using an in-house Modelica library which was specifically developed to promote reusability of components.

Both downcomer and riser are the components which regulate the mass flow rate of the system. As detailed in the works of Ling (2015) and Qiao (2015) only momentum equation is critical for such components. This assumption is reasonable because the heat exchangers have higher thermal capacitance compared to them. Hence mass or energy storage is ignored in the modeling to improve computational time without significant change in results.

The finite volume discretization of momentum equation is described in Elmqvist and Tummescheit et al (2003). For the lumped control volume of downcomer (Figure 4), by equating the inlet and outlet mass flow rates, we obtain

$$\frac{d\dot{m}}{dt}L_t = A(p_a - p_b) - \frac{1}{2}\frac{\dot{m}^2}{\rho A^2}fSL_t - A\rho g\Delta z \tag{9}$$

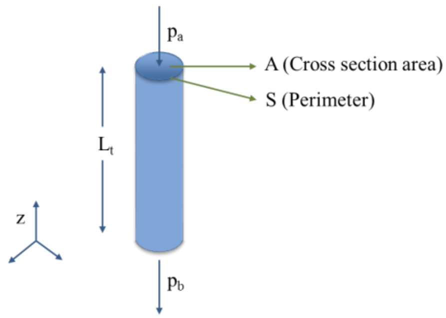

Figure 4: Control volume of downcomer

For the downcomer, the outlet (b) is below the inlet (a) in height and hence $\Delta z = -L_t$ while for the riser $\Delta z = L_t$. The Fanning friction factor is calculated using correlation developed by Gronnerud (1979). The mass flow rate is initialized by using experimental data since the equation calculates only its rate of change with time.

5. RESULTS AND DISCUSSION

The modeling for thermosiphon involved an initial condition, obtained from experimental data, of the PCM to be molten at 42°C. The simulation is run until the temperature of the outermost finite volume ring reaches 35°C. Since the container of PCM is made of low-conductivity plastic, the assumption that outer ring of the cylindrical PCM block has adiabatic boundary condition (Equation 4) is reasonable.

Mass flow rate for the thermosiphon operation mode is given in Figure 5. As can be seen from Figure 1, mass flow meter (MFM) is bypassed during thermosiphon mode of operation in order to reduce the flow resistance and hence experimental values for mass flow rate are not available. However, values for airside inlet and outlet temperatures for airside heat exchanger as well as the volume flow rate for the fan are available. Hence by equating these values to refrigerant side, mass flow rate of the refrigerant at a particular time interval is calculated to be 0.4 g/s. Since mass flow rate is not measured for the set-up, this number only serves as a check for correct order of magnitude.

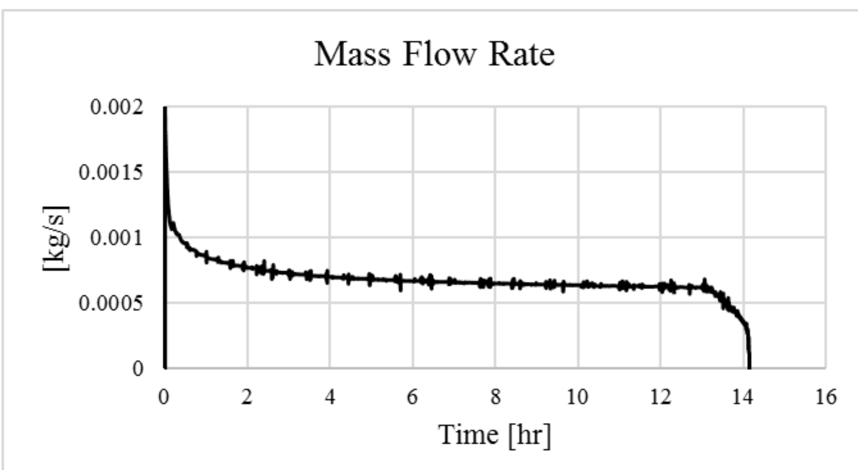

Figure 5: Mass Flow Rate for thermosiphon mode

Heat rejection from the PCM is also plotted against time in Figure 6. For comparison, values from experiment are overlaid. The thermosiphon mode of operation is terminated at 500 minutes (~ 8 hours) in the experiment. Another comparison carried out is the refrigerant side inlet temperature for the airside heat exchanger. This is the only instream thermocouple which is not bypassed during thermosiphon mode and hence is used for comparison (Figure 7).

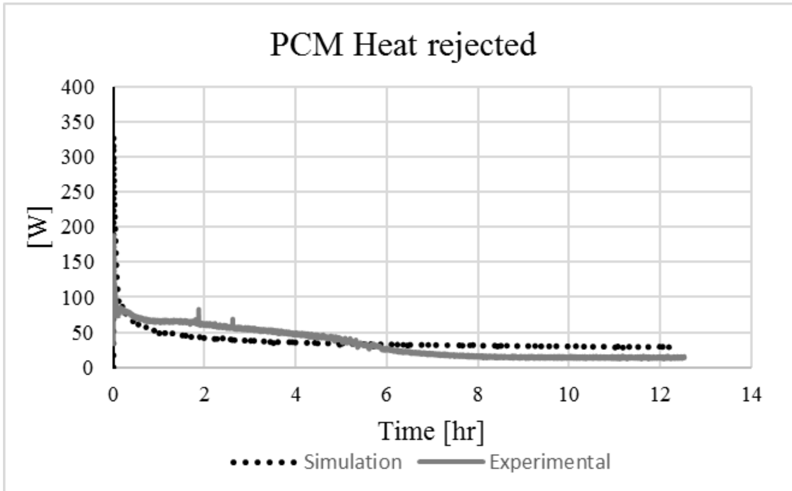

Figure 6: Rate of heat rejection by thermosiphon

The runtime for thermosiphon is taken as time for the outermost ring of finite volume to reach a temperature of 35°C. One of the objectives of thermosiphon modeling is to improve upon this recharge time. PCM thermal properties are critical for this performance. Table 1 provides thermal properties of all the materials available for consideration.

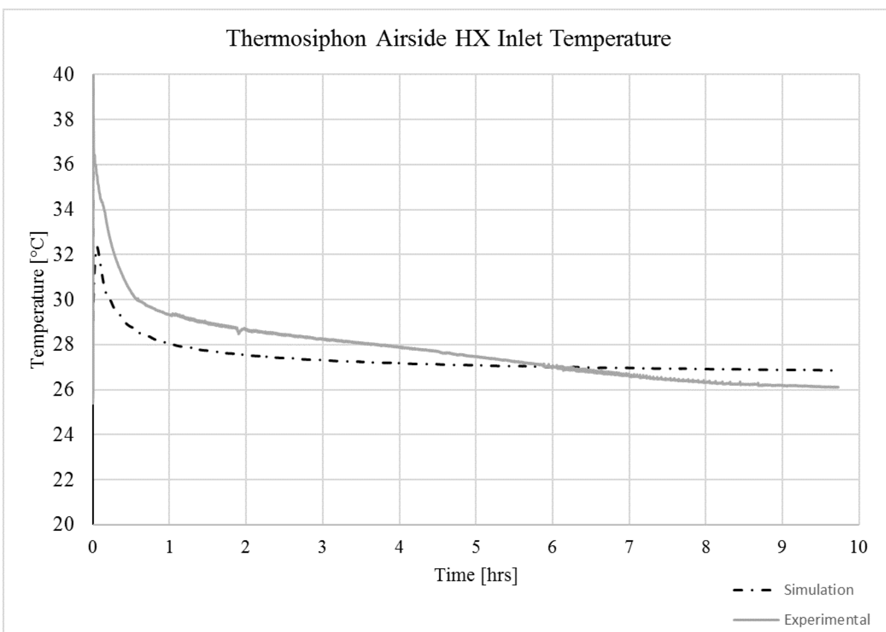

Figure 7: Comparison of temperature between simulation and experimental data

The recharge time in this case is 13 hours for the base case with Pure PCM. This is significantly higher than the experimental value of 8.3 hours. The deviation is due to the assumption of adiabatic PCM container. In the real case, the PCM block is not fully insulated and the heat losses through the PCM container results in faster recharge time for the PCM. However, for the present situation, simplistic approach has been adopted. The recharge time is calculated as the time taken for the thermosiphon to freeze only 81.7% of the PCM (as seen in Figure 8). This definition implies an assumption that in all situations, the percentage of heat loss to ambient will be constant.

Table 1: Phase Change Material Properties

Graphite Bulk Density [kg/m^3]	**0**	**11**	**23**	**50**	**100**	**143**
Melting Point (°C)	37	37	37	37	37	37
Latent Heat (kJ/kg)	210	208	205	200	176	145
Thermal Conductivity liquid (W/m-K)	0.15	1.1	2.3	4.7	9.6	20.2
Thermal Conductivity solid (W/m-K)	0.25	1.1	2.3	4.7	9.6	20.2
Specific Heat Capacity liquid (J/kg-K)	2630	2621	2610	2588	2545	2509
Specific Heat Capacity solid (J/kg-K)	2210	2203	2195	2177	2144	2115
Density liquid (kg/m^3)	840	846.9	854.5	871.4	902.8	929.8
Density solid (kg/m^3)	920	926.5	933.6	949.6	979.3	1005.0

The PCM block is modeled with 25 rings of equal thickness. However, the mass of PCM is distributed more towards the outside. The cutoff radius for 81.7% of mass from the center can be calculated from Equation 10. Its value comes out to be 0.0211 m. Hence the time period when 23rd ring, starts to melt is taken as the total thermosiphon period.

$$\frac{m}{\rho \pi L_t} * 0.817 = r_c^2 - r_i^2 \tag{10}$$

The new recharge times with this definition are shown in Figure 9. The recharge time for the case with Pure PCM is 10 hours which is closer to the experimental result. The spiral refrigerant tube in the condenser, results in lesser thermal resistance between the PCM and refrigerant leading to faster heat rejection. However, accurate modeling of a three dimensional heat exchanger with spiral tube for its transient behavior is computationally expensive and not the objective of this study.

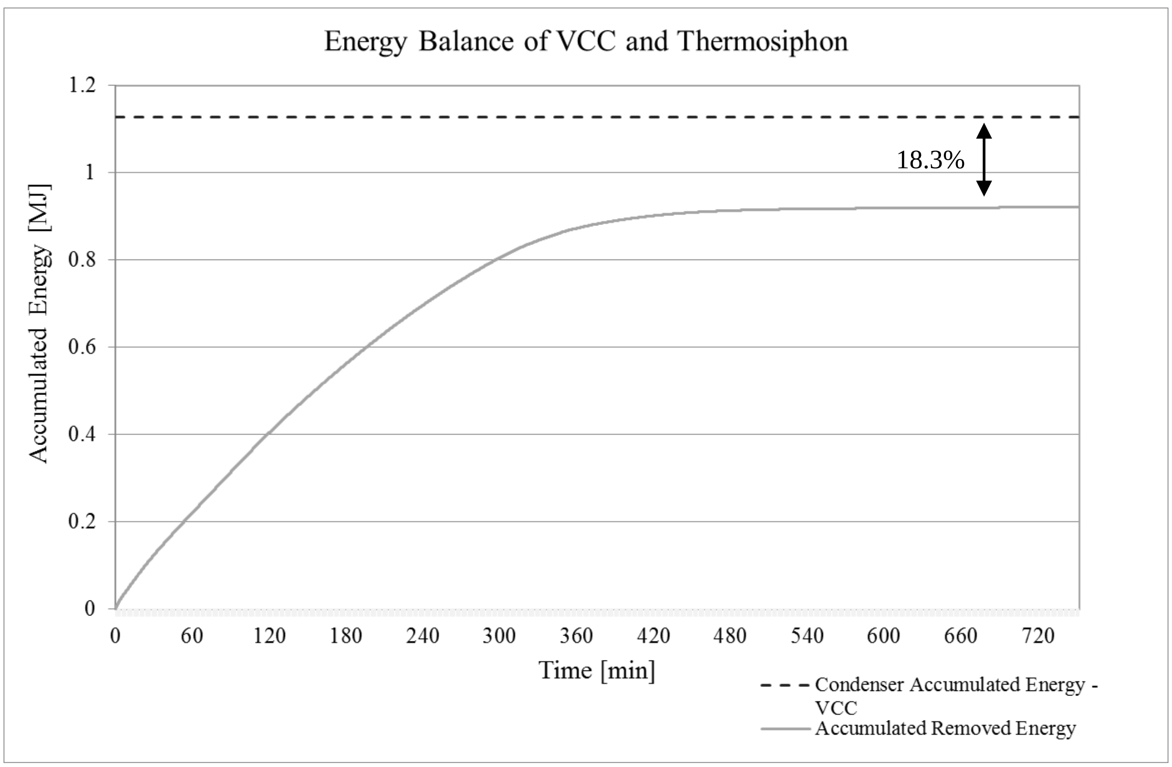

Figure 8: Energy rejection by thermosiphon

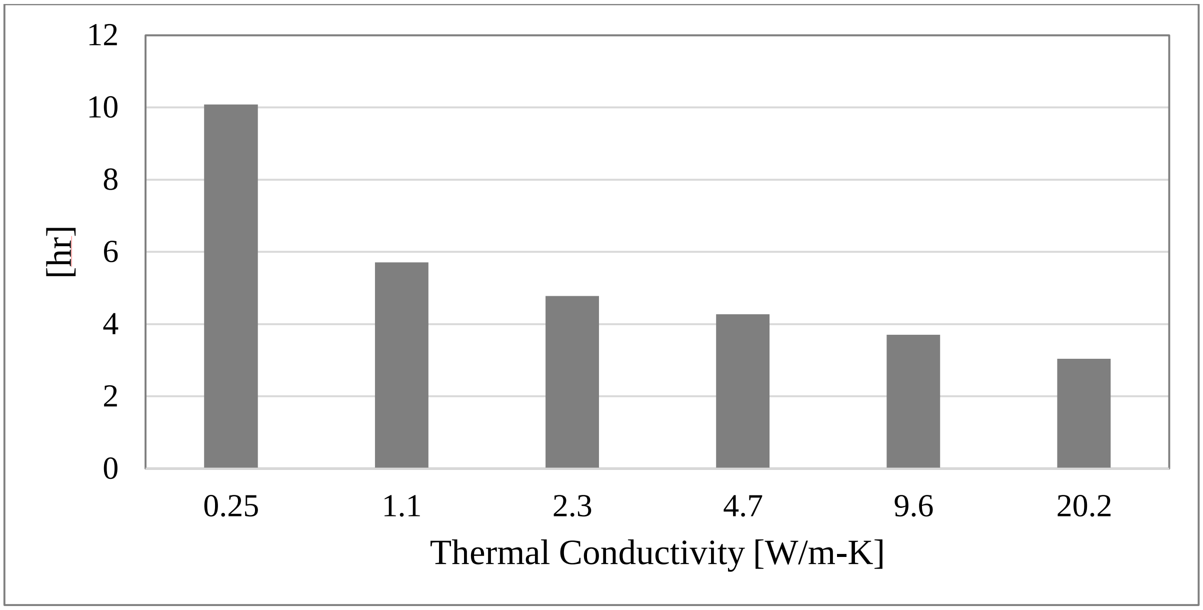

Figure 9: Recharge time for 81.7% heat loss

Increase in thermal conductivity by graphite addition reduces the latent heat capacity of the PCM but allows higher heat transfer between the refrigerant and PCM block for faster recharge time. Hence there is a critical value up to which the graphite addition has to be done so as to have an effective compact thermal storage. The heat storage capacity of each case is plotted in Figure 10. The parameter for deciding which material suits best for thermosiphon operation is the heat rejection rate. This is evaluated by dividing the net heat rejected from Figure 10 by the corresponding recharge time from Figure 9. The results are shown in Figure 11.

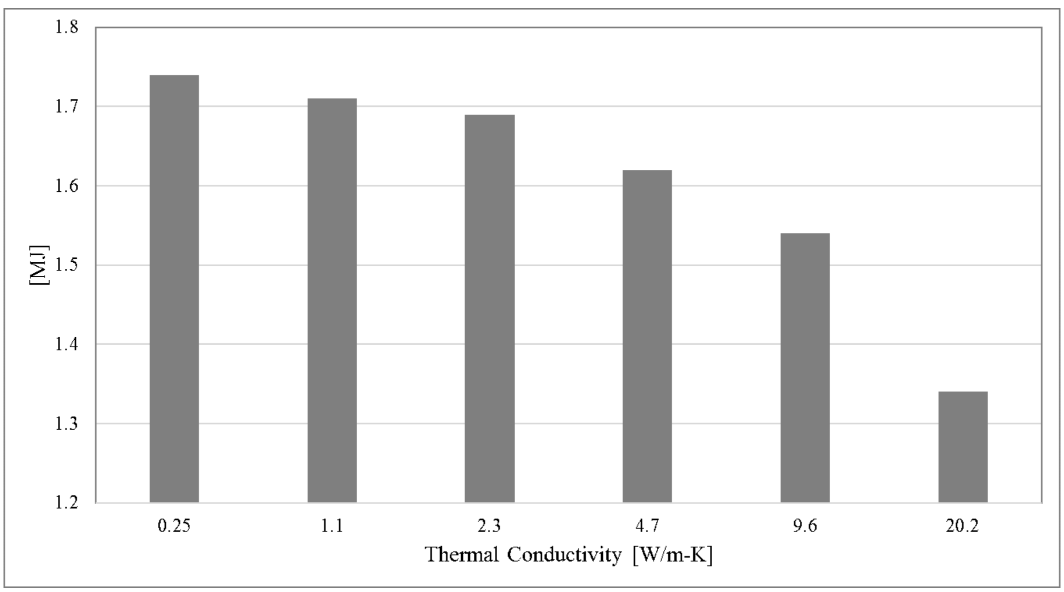

Figure 10: Net heat rejected during thermosiphon mode

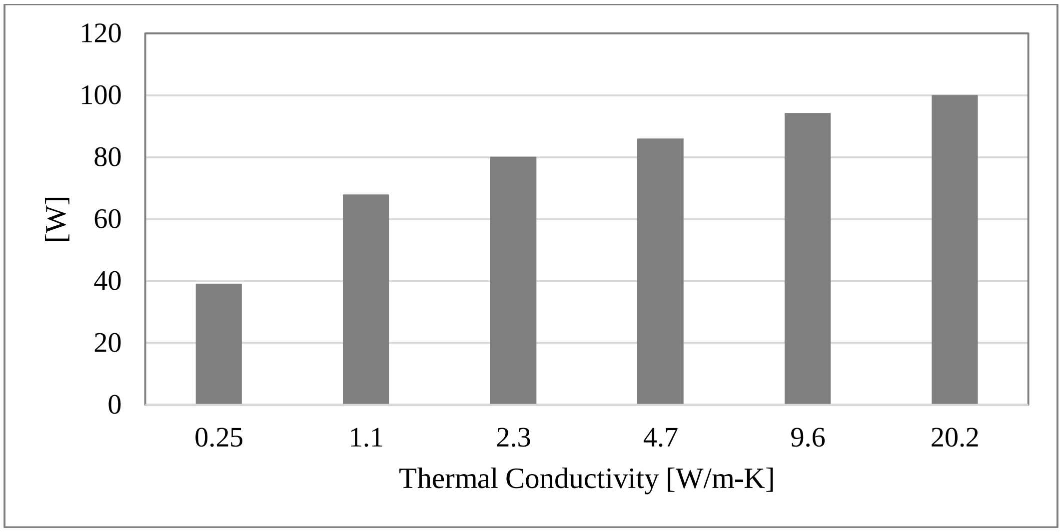

Figure 11: Rate of heat rejection from thermosiphon

6. CONCLUSIONS

This paper presents an optimization study of a gravity assisted thermosiphon which extracts heat from a molten PCM heat exchanger. The objective is to understand the effect of various PCM and choose the most favorable one by tradeoff between minimizing weight and having faster recharge time. The RoCo operating time for the current prototype is 2 hours with 8 hours needed for its thermal recharge from thermosiphon operation. The new graphite enhanced PCM is expected to bring down the recharge time of thermosiphon by half to aid multiple operations of RoCo during the day. It can be observed from simulations that there is a definite improvement in the thermal recharge time for the operation of RoCo with increase in the graphite percentage in PCM. By switching to materials of higher graphite bulk densities, it is possible to reduce the recharge time to 30% of its current value. Since the materials with bulk densities of 100 kg/m^3 and 143 kg/m^3 have significantly less latent heat capacity, their usage would imply a heavier PCM storage. Hence for the next prototype material with bulk densities of 50 kg/m^3 has been selected.

NOMENCLATURE

A	Area	(m^2)
c	Specific heat capacity	(J/kg-K)
E	Specific Energy	(J/m^3)
f	Fanning friction factor	(-)
g	Acceleration due to gravity	(m/s^2)
k	Thermal Conductivity	(W/m-K)
L	Latent heat of melting	(J/kg)
L_t	Tube length	(m)
m	Mass	(kg)
$\dot{m}$	Mass flow rate	(kg/s)
p	Pressure	(Pa)
q	Heat flux across boundary	(W/m^2)
r	Radius	(m)
ρ	Density	(kg/m^3)
S	Perimeter	(m)

t	Time	(s)
T	Temperature	(K)
V	Volume	(m^3)
z	difference in height of inlet and outlet	(m)

Subscript

c	Cutoff
i	Inner
init	Initial
j	Control Volume index
L	Liquid
m	Melting point
n	Timestep number
o	Outer
p	Constant Pressure
S	Solid
t	Refrigerant tube

REFERENCES

1. Alexiades, V., Solomon, A (1993). *Mathematical Modeling of Melting and Freezing Processes*. Hemisphere Publishing Corporation
2. Ling, J., Bhanot, V., et al (2015). Transient simulation of heat pumps using low global warming potential refrigerants. Science and Technology for the Built Environment. Vol 21(5), 658-665
3. Dhumane, R., Ling, J., et al (2016). Transient Multiphysics Modeling of a Robotic Personal Air-Conditioning Device. *16th International Refrigeration and Air Conditioning Conference, Purdue, Indiana, USA*
4. Elmqvist, H., Tummerscheit, H., et al (2003). Object Oriented Modeling of Thermo-Fluid Systems. *Proceedings of 3rd International Modelica Conference, Linkoping, Sweden*. 269-286
5. Gronnerud, R., Investigation of liquid hold-up, flow-resistance and heat transfer in circulation type evaporators, part IV: two-phase flow resistance in boiling refrigerants. Annexe 1972-1, Bull. De. de l'Inst. du Froid
6. Hoyt, T., Kwang H., et al (2005). Energy savings from extended air temperature setpoints and reductions in room air mixing. *International Conference on Environmental Ergonomics 2009, Boston, USA*
7. Leonhardt, C., Muller D., et al (2009). Modelling of Residential Heating Systems using a Phase Change Material Storage System. *Proceedings 7th Modelica Conference, Como, Italy*
8. Qiao, H., Aute, V., et al (2015). Transient modeling of a flash tank vapor injection heat pump system – Part I: Model development. *International Journal of Refrigeration*, Vol 49, 169-182

ACKNOWLEDGEMENT

The authors are grateful for ARPA-E for funding the project with Award Number DE-AR0000530. They would also like to acknowledge the contributions of colleagues Anne Mallow and Kyle Gluesenkamp from Oak Ridge National Laboratory for providing experimental data for the graphite enhanced PCM.